

The association between transition metal components of PM_{2.5} and lung function
and density: The Multi-Ethnic Study of Atherosclerosis.

Mark D. Sullivan

A thesis

submitted in partial fulfillment of the

requirements for the degree of

Master of Public Health

University of Washington

2012

Committee:

Sverre Vedal

Joel Kaufman

Degree Program:

Environmental & Occupational Health Sciences

Introduction:

Lung diseases as a whole are the third leading cause of mortality in the US, with an estimated 16 million Americans living with chronic lung disease such as asthma and chronic obstructive pulmonary disease (1). The etiologies of chronic lung disease are wide-ranging from occupational, environmental and modifiable exposures such as smoking (2-4). While some risk factors for development and progression of chronic lung disease are well known, the role of chronic low-level exposure to air pollution association in lung disease remains uncertain.

Particulate matter (PM) is one of six common air pollutants (AP) identified by the Clean Air Act and monitored by the EPA which is responsible for setting National Ambient Air Quality Standards. Health effects related to Inhalable Particles of less than 10 microns in diameter (PM_{10}), and Fine Particulates of less than 2.5 microns ($PM_{2.5}$) are of most concern as both fractions are capable of reaching the level of the alveoli where direct pulmonary or vascular endothelial damage is believed to occur (5). PM is composed of numerous chemicals which are as varied as are their sources of origin and range from pure elements to organic dusts. PM burden also differs widely across the US, with the heaviest contributors to $PM_{2.5}$ being unpaved road dust, agricultural soil, wildfires, coal combustion, residential wood combustion and diesel exhaust (6). Individually, many of these compounds and elements have been shown to be toxic based on existing data from animal studies and human epidemiology (7, 8).

Transition metals (TM's) represent a small portion of elemental species found within $PM_{2.5}$, but are important as they have high potential for reactivity in

vivo (9). TM exposures have been shown to react with cellular components leading to creation of reactive oxygen species (ROS) such as superoxide anion, hydrogen peroxide, and hydroxyl radical or contribute to depletion of glutathione and protein-bound sulfhydryls, all of which may increase potential for end organ tissue damage (9, 10). TM's have also been found to directly stimulate inflammatory mediator production, alter signaling cascades and act at the level of gene transcription regulation(10, 11). Because of their ubiquitous distribution in PM_{2.5} and potential for metal-induced ROS formation, transition metals are of increasing interest in their possible role in the development of lung disease (6, 12). For this study we chose four transition metal elements for their known association with lung disease; Chromium, Cobalt, Cadmium and Nickel. Each has been linked to disease such as cancer, nephropathy, and cardiomyopathy and all are highly regulated by OSHA for occupational health and safety purposes. Nickel, Chromium, Cadmium and Cobalt components of tobacco smoke, and are being examined as specific factors for association with development of chronic lung disease, cancer and COPD (13-15).

In vitro animal studies of Cobalt and Chromium-6 exposures have shown these metals covalently bond protein, DNA, and also interact with signaling pathways leading to up regulation of p53 and ultimately apoptosis (15, 16). Cadmium has been shown to down regulate the Cystic Fibrosis Trans-membrane Conductance Regulator (CFTR) leading to impaired regulation of the airways surface and higher potential for subsequent inflammation and infection (17). Finally, Nickel has been demonstrated to produce brisk alveolar cellular and chemokine inflammatory response and subsequently generated ROS produce a hypoxic state

within the cell that may favor tumorigenesis or apoptosis (18, 19).

Smoking is a well known cause of Chronic Obstructive Lung Disease (COPD), but an increasing trend of COPD is being observed in never-smokers with implication that outdoor air pollution may be a contributor to the increasing prevalence of this disease (20). COPD is a clinical diagnosis indicated by a post-bronchodilator decrease in the Forced Expiratory Volume in 1 second (FEV1) to Forced Vital Capacity (FVC) ratio of less than 0.70 in adults, with severity grade based on the % predicted value of FEV1 decline (21). However CT scan imaging techniques are now being investigated as a useful modality for identifying emphysematous lung changes as a method of identifying COPD. Recently, Hoffman et al demonstrated reproducibility and validity of using EBT and MDCT cardiac imaging modalities from the MESA study to identify low attenuation areas (LAA) consistent with subclinical emphysema (“percent emphysema”) in patients within the MESA-Lung cohort (22).

Obstructive lung disease etiology is a growing concern due to increasing incidence and prevalence in never smokers. The reactive nature of transition metals, and their presence in PM2.5 may point to an association with prevalence of obstructive lung disease. In this cross sectional study using the MESA Air population based cohort, we intend to investigate whether exposure to ambient air pollution levels of 4 specific transition metals (Ni, Cr, Cd, Co) is associated with decreased lung density by CT scan and decreased lung function by spirometry.

Research Hypotheses:

Primary: Exposure to ambient concentrations of PM_{2.5} transition metals (Cadmium, Cobalt, Chromium and Nickel) is associated with decreased lung density (AKA increased percent low attenuation) as measured by Computed Tomography.

Secondary: Exposure to ambient concentrations of PM_{2.5} transition metals (Cadmium, Cobalt, Chromium and Nickel) is associated with airways obstruction as measured by spirometry.

Methods:Study Setting:

The MESA Classic study was initiated in 1999 and is a multi-center cohort of more than 6,814 participants aged 45 to 84 years followed for over 10 years with the principle goal to investigate prevalence of subclinical and subsequent development of overt cardiovascular disease events (peripheral artery disease, acute myocardial infarction, congestive heart failure and stroke) with mortality. This study has compiled data from clinical evaluation, diagnostic imaging and other clinical studies performed at 5 exam intervals starting in 2000-2002 with baseline Exam 1 through Exam 5 completed by Dec 2011. The cohort was recruited from 6 field sites: Forsyth County, NC; Northern Manhattan and the Bronx, NY; Baltimore City and Baltimore County, MD; St. Paul, MN; Chicago and the village of Maywood, IL; and Los Angeles County, CA. The Multi-Ethnic Study of Atherosclerosis and Air Pollution (MESA Air) is an ancillary study of MESA and began in 2004 to investigate

the relationship between air pollution exposures and the progression of subclinical atherosclerosis and the incidence of cardiovascular disease.

Study Subject Selection:

Participants within the MESA Classic study were recruited into MESA Air at MESA exam 4 with initially 5,479 (93%) agreeing to participate, but an additional 186 enrolled at exam 5. MESA Air also enrolled 257 “New Recruits” at exam 4; 490 participants from the MESA Family ancillary study at exams 3 and 4; and 615 participants from the MESA Neighborhood Study with already obtained MESA classic exam 1 data for a total combined cohort of 7,031 (table 1). During this study period participants underwent physical and other medical exams at specified dates, during which metrics such as coronary artery or full chest CT, and spirometry were performed (table 2).

TABLE 1: Recruitment sources into MESA Air

Recruitment source	Total N	Exam at which joined MESA "Classic"	Exam at which they joined MESA Air
Classic	5669	1	4 and 5
New Recruits	257	Directly enrolled	4
Family	490	NA	3 and 4
Neighborhood	615	1	NA
	7031		

TABLE 2: Exam dates and obtained studies

MESA Recruits	Exam 1 Jul00- Aug02 (24 months)	Exam 2 Sep02- Feb04 (18 Months)	Exam 3 Mar04- Sep05 (18 Months)	Exam 4 Sep05- May07 (21 Months)	Exam 5 Apr10- Dec11 (21 Months)
Classic	CT Coronary (Chest)		Spirometry	Spirometry	
Air:New Recruits			CT Coronary (Chest) Spirometry	CT Coronary (Chest) Spirometry	
Family			CT Coronary (Chest) Spirometry	CT Coronary (Chest) Spirometry	
Neighborhood	CT Coronary (Chest)		Spirometry	Spirometry	

Exposure Data Collection:

National (Spatial) estimates of Ni, Cr, Co, Cd levels were obtained from one-year averages of data from 2009 and 2010 as measured by the EPA's Interagency Monitoring for Protected Visual Environments (IMPROVE) and Chemical Speciation Network (CSN). The IMPROVE monitors are a nation-wide network of air quality monitors located mostly in National Parks and other similarly remote areas, put in place to assess and regulate pollution related visibility limitations. The CSN monitors are located in urban areas and were combined with the IMPROVE monitor data to provide a collection of pollution measurements that spatially are evenly dispersed throughout the lower 48 states. TM exposure concentration at each participant's address was predicted using a land use regression model (i.e., the

mean model). Over 200 geographic covariates from the following categories: multiple indirect measures of traffic, population density, land use, satellite-based vegetative index, nearby pollutant emissions based on emissions inventories, and distance to major sources of pollution were included in the model. Partial least squares (PLS) techniques were used to select relevant land use variables for the mean model. The model, in which monitor concentrations were regressed on the PLS components, was fit using maximum likelihood. Universal kriging was used to model the remaining spatial structure in the residuals from the mean model.

Nearest monitor estimates for Ni, Cr, Co, Cd levels were obtained every other week from 3 to 7 fixed monitors in each MESA city for the years from 2006-2008. Average concentrations were then determined for each monitor that produced greater than 50% annual observations (≥ 13 out of 26) and at least 2/3 collection years represented. TM estimate for each MESA Air subject was subsequently assigned by nearest monitor to baseline address at enrollment exam.

Endpoint Data Collection:

Computed Tomography Scanning Protocols

MESA Cardiac CT Protocol: Cardiac scans were performed under a standardized protocol by designated, MESA-certified, experienced radiology technologists, under the supervision of the reading center co-investigator (23). Two sequential axial scans with prospective cardiac gating were performed in succession on each participant at each visit. The participant was asked to take three deep breaths and then hold lung volume at end-inspiration. At the time of baseline

scanning, three MESA sites had MDCT scanners and the other three had EBT scanners. For MDCT scanners, the mAs was increased by 25% for participants who weighed >220 lbs.

Full-Lung Chest CT Protocol: The MESA MDCT full-lung chest protocol has been previously described in a validation study by Carr et al 2009, and was similar to the NHLBI-funded National Lung Screening Trial protocol except for a slightly higher effective dose to better image the lung parenchyma (23). The scan imaged the chest from 1 cm above the lung apices to 1 cm below the diaphragm, following instruction for a very deep breath hold. Following the MESA cardiac CT protocol, the mAs was increased by 25% for subjects who weighed > 220 lbs.

Lung Density Measures

Protocols used for cardiac CT, full chest CT and subsequent lung density measurements were previously described in the MESA Lung CT validation study (22, 23). Images were assigned to one of several trained image analysts who assessed lung density using the Pulmonary Analysis Software Suite (PASS) which was used in the NHLBI-funded National Emphysema Treatment Trial (22, 24, 25) and was modified for use with cardiac scans. Percent emphysema was reported as the percentage of the total voxels in the whole, apical and basal lung that fell below -950, -910, and -850 HU. These thresholds were set to identify severe, moderate and mild emphysema-like lung regions respectively. Lung holes were defined as connected voxels within a scanned slice falling below -950, -910, or -850 based upon the studies of Mishima et al (26, 27). Attenuation of air was measured outside the

chest on a random sample of scans to confirm scanner calibration at -1,000 HU.

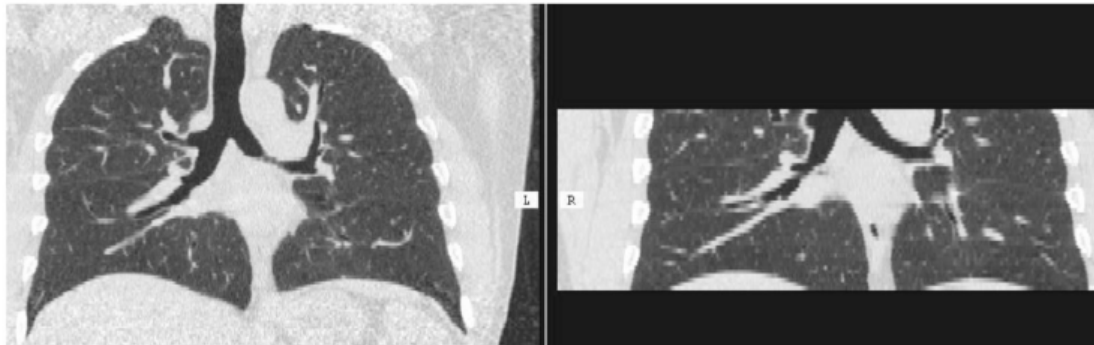


Fig 1a. Lung windows from full chest CT vs cardiac CT exams side by side comparison (22).

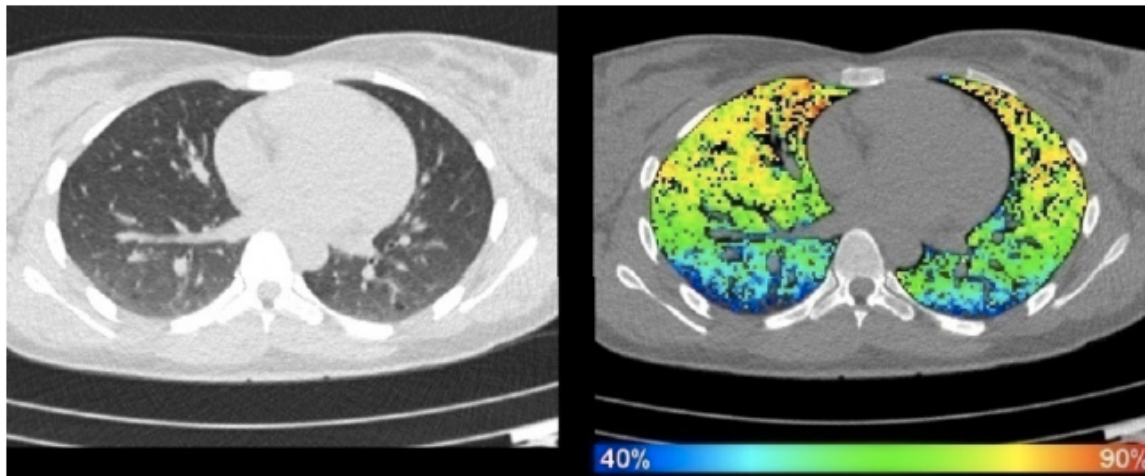


Fig 1b. Number of voxels with X-ray attenuation of < -950 HU (reprinted with permission from Graham Barr)

Spirometry:

Spirometry data was collected using a SensorMedics model 1022 rolling-barrel spirometer fitted with a digital volume encoder, temperature sensor and RS232 serial computer interface. The system provides an automated assessment of test quality with immediate feedback to the technician allowing interaction between the spirometry technician and subject. All participants underwent uniform standardized spirometry, performed by centrally trained or locally certified MESA

technicians as part of Exam 3 and 4. All testing was performed in accordance with ATS guidelines (28). Each participant performed maneuvers in a seated position following the standardized protocol up to eight times or until at least three acceptable and reproducible maneuvers were obtained. The software assists in the determination of acceptable and reproducible maneuvers. MESA-Lung Spirometry Completion Forms indicate testing position, client effort, reactions, and any supplemental comments such as participant cooperation, leak-mouthpiece, false start, or early termination of expiration.

Study Aims:

Overview:

This study was designed to assess the association between lung airways disease and exposure to PM_{2.5} components of the selected transition metal species Cobalt, Chromium, Nickel and Cadmium. We utilized available cardiac, full chest CT scans and spirometry data from the full MESA Air cohort collected from baseline exam 1 and follow up exams 3 and 4 (table 2). Transition metal exposure data from national and nearest monitor estimates were assigned to baseline address and merged with CT and spirometry data sets for analysis. We proceeded with analysis assuming that the relationship between the geographic variables and the monitor concentrations of transition metals did not change meaningfully between our predicted baseline exam dates and actual dates of TM measurement. The primary hypothesis is that increased transition metal concentrations are associated with decreased lung density as evidenced by LAA. Secondary analysis to assess

association of transition metal concentrations with spirometry measurements of FEV1, FVC, and the FEV1/FVC ratio was designed to assess coherence with the primary hypothesis. LAA and spirometry endpoints were regressed on TM estimated from either a spatial model or nearest monitor for base model (gender, age, height, weight, bmi), full model (+ smoking status, pack years, asthma history, income level, occupation, education) and full model + either PM2.5 or city adjustment terms (Appendix A).

Hypothesis testing:

Study Sample: All MESA Air, Family and New Recruit cohort participants with baseline Exam 1 CT scan and Exam 3 or Exam 4 CT scan and Spirometry.

Exposure Variables: Predicted PM_{2.5} transition metal concentrations for MESA study participants based on national spatial models developed in National Particle Component Toxicity (NPACT), and nearest monitor estimates from fixed MESA city air monitors.

Outcome Variables: Lung density measurements from Exam 1 and Exam 3/4, Spirometry values (FEV1, FVC, FEV1/FVC ratio) from Exam 3/4.

Covariates: race, age, weight, height, gender, BMI, smoking status, smoking pack years, asthma history, occupation, education, income.

Possible Confounders: PM2.5, unmeasured city-associating factors

Power:

Utilizing the R statistical software “pwr.f2.test” package using the 12 predictors previously listed, a sample size of $n=7,031$, and alpha of 0.05 (see appendix A) we were able to determine the effect size (F2) for our study at 50%, 80% and 90% power. We utilized the equation $F2 = R^2_{total} - R^2_{model} / 1 - R^2_{total}$ to determine the detectable difference from our R^2_{total} above the model population $R^2 = 0.2159$ (R^2_{model}) value reported by Grydeland et al for quantitative CT analysis of emphysema (29, 30)(Appendix B). Detectable % change in R^2 LAA for our total model - 0.2159 was 0.11% (i.e., 0.0011) at 50% power, 0.19% at 80% power, and 0.24% at 90% power for inclusion of a single transition metal variable in the model. Therefore we have sufficient power to detect less than a 1% difference above the R^2_{model} that might be expected from an effect of transition metals.

Statistical Methods:

Baseline descriptive statistics characterizing the study population were performed for the outcome variables, exposure variables, and the selected covariates. This included data distribution measures for continuous measures of mean + std deviation, median, quartiles, and frequency statistics for discrete measures.

Primary analysis: We performed multiple linear regression analysis of LAA on study subject predicted $PM_{2.5}$ transition metal concentrations at the home residence utilizing spatial model and nearest monitor estimates of exposure.

Secondary analysis: We performed multiple linear regression analysis of FEV1, FVC and FEV1/FVC values on study subject predicted PM_{2.5} transition metal spatial model and nearest monitor estimates of exposure.

Sensitivity and exploratory analyses:

- 1) Exploratory analysis of associations of %LAA and spirometry with predicted concentrations of transition metals was carried out for race, gender, and enrollment city site.
- 2) Alternative specification of transition metal effects, for example, assessing whether transition metals modify the PM_{2.5} effect, and models controlling transition metal effects for effects of total PM_{2.5}, was explored.
- 3) Sensitivity analysis of PM_{2.5} effect alone, and controlling for city site on %LAA and Spirometry were performed.

Model Diagnostics:

- 1) Appropriate linear versus non-linear model fitting was assessed by residuals analysis and Q-Q plots.
- 2) Data was examined for influential outliers by Cook's point analysis.

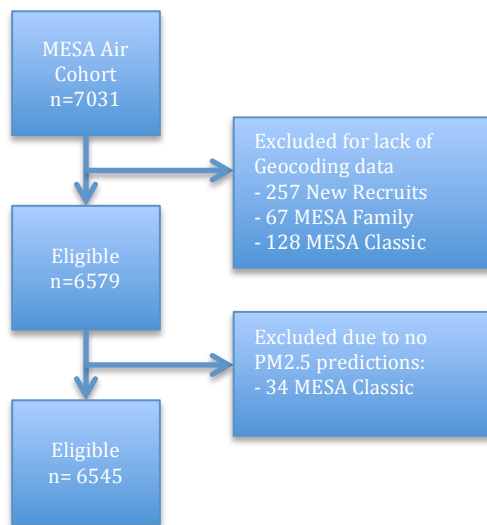
Results:

Analysis Sample:

The MESA air cohort is composed of several subsets from the MESA Classic and Family cohorts and also 257 "New Recruits" directly into MESA Air to bring a total n=7031. Exposure estimates from the spatial and nearest fixed monitors were assigned to each MESA air participant per baseline exam address, and this data

merged with baseline exam CT data and spirometry data for each participant. Further merging of PM2.5 exposure data was done to obtain a complete data set for regression analysis. Unfortunately there was no TM data obtained for any of the New Recruit subjects, therefore leading to their exclusion from analysis. Additional exclusions were due to lack of PM2.5 data, and in the secondary analysis lack of spirometry data for analysis (fig 2).

a) LAA Analysis:



b) Spirometry Analysis:

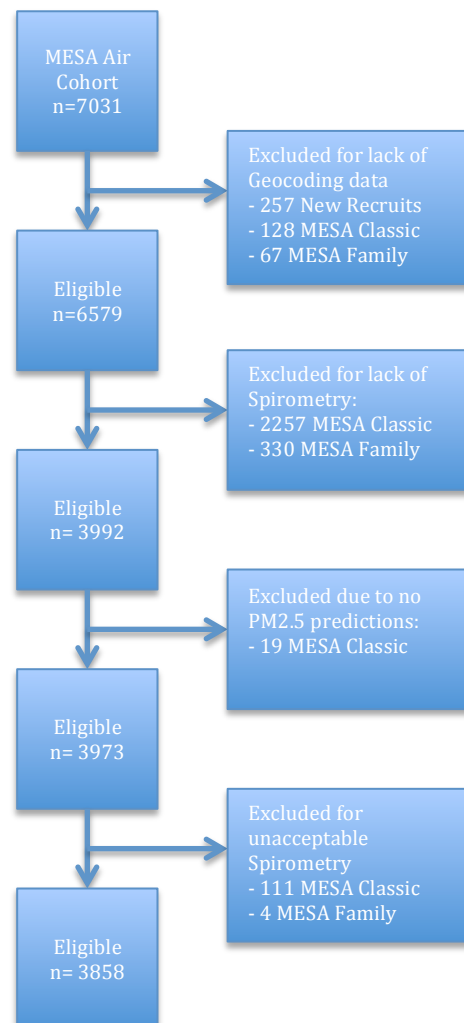


Fig 2. Exclusion flowchart for MESA Air cohort analysis of LAA and Spirometry

Demographics

Characteristics of the entire MESA Air cohort compared to the final sample sets for analysis are shown in table 3. Despite the decrease in subject number from the original cohort, the demographics distributions remain similar for LAA and Spirometry analysis in regard to mean age gender, and race. Additional information such as height, weight, BMI, smoking status, pack years of smoking and asthma history remained similar as well (table 3).

Table 3. Demographics

	%LAA n=6545	FEV1 n= 3858	MESA Air Cohort n=7031
Means	0.74(0.085)	2.38 L (0.73)	
Age	61 (10.11)	65 (9.84)	61(10.09)
Age Group			
40-44	16 (0.3%)	4 (0.1%)	16(0.2%)
45-54	1957 (29.9%)	1209 (31.3%)	2066(29.4%)
55-64	1874 (28.6%)	1110(28.8%%)	2054(29.2%)
65-74	1874 (28.6%)	1116 (28.9%)	2013(28.6%)
75-84	824 (12.6%)	419(10.9%)	875(12.5%)
>85	0	0	3(0.04%)
Gender			
Female	3479 (54%)	1969 (51%)	3726(53%)
Male	3066 (46%)	1889 (49%)	3305(47%)
Race			
African Am	1870 (28.5%)	968 (25.1%)	1969(28%)
Asian	717 (11%)	611 (15.8%)	703(10%)

Hispanic	1556 (23.8%)	948 (24.6%)	1687(24%)
White	2402 (36.7%)	1331 (34.5%)	2672(38%)
Weight lbs	170.5 (38.18)	171.2 (38.49)	174.7(38.4)
Height cm	166.1 (10.01)	165.8 (10.03)	166.5(10.0)
BMI	27.64 (5.51)	28.13 (5.44)	27.7(5.6)
Pack Years	10.80 (21.7)	11.98 (21.94)	10.95(21.6)
Smoking Status			
Never	3321 (50.7%)	2030 (52.6%)	3558(50.6%)
Former	2370 (36.2%)	1356 (35.1%)	2570 (36.6%)
Current	854 (13.1%)	472 (12.23%)	903(12.8%)
Asthma			
No	5894 (90.05%)	3413 (88.5%)	6328(90%)
Yes	651 (9.95%)	445(11.5%)	703(10%)

Table 4. Demographics of analysis cohort compared to full MESA Air cohort. Reported as mean values (standard deviation or percent of total).

Descriptive Analysis

The distributions of Ni and Cr from spatial estimates were investigated with Ni showing a bimodal distribution whereas Cr is a single distribution. This bimodal distribution has been attributed to residential use of residual oil fuel in New York (NY) which has been shown to produce higher ambient Ni level on combustion (31). As such, Ni estimates were also examined excluding NY subjects and show a single, normally approximated distribution though slightly right skewed (Fig 3a). Cr distribution also approximated normal with right skewing (Fig 3c). Boxplots show comparative Ni and Cr levels within each MESA city, and highlight the Ni level elevation in NY compared to lower levels in the other MESA cities (Fig 3b and d).

Distributions of TM's for the nearest monitor analysis were also investigated and shown in fig 4. These do not follow a continuous distribution pattern as for the spatial model since participants are assigned a TM exposure value based on that recorded from their nearest monitor at baseline address.

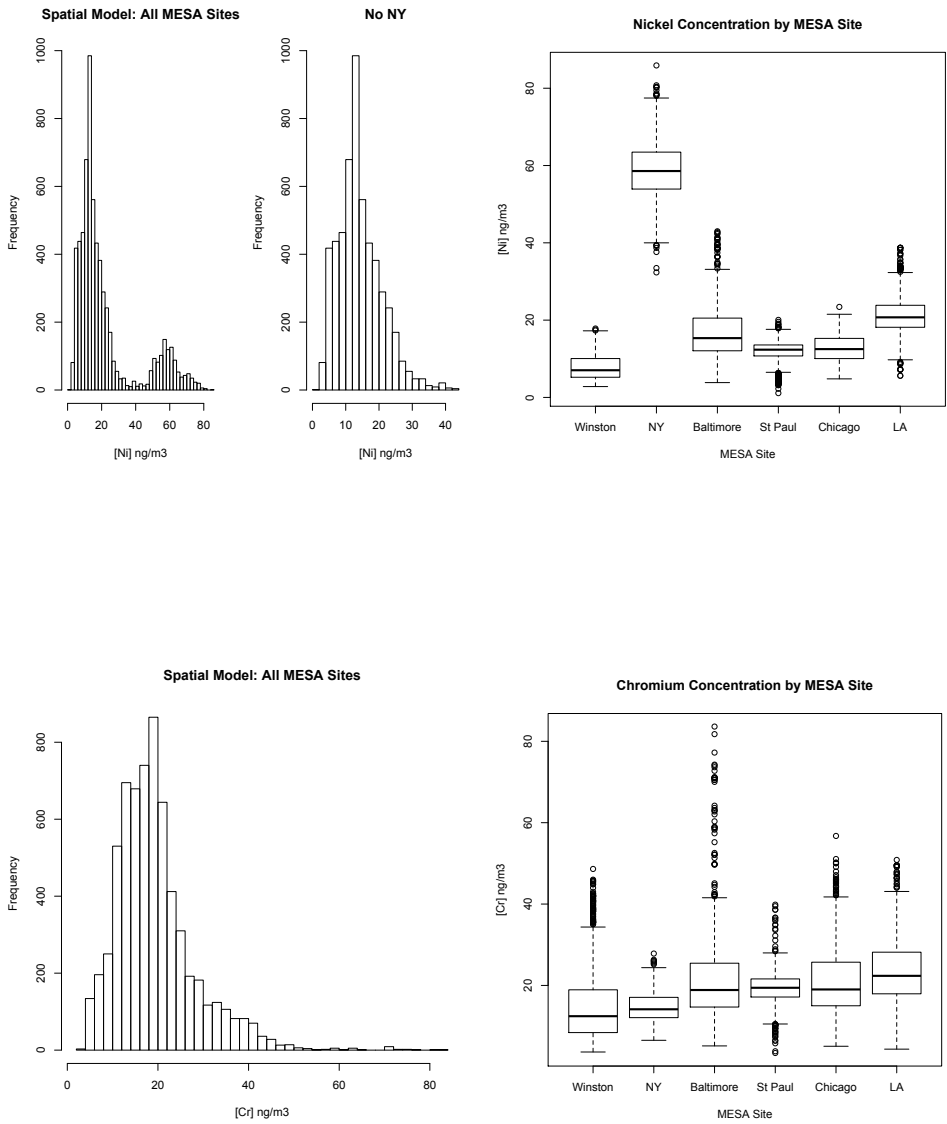


Fig 3. a) Distribution of Nickel predicted from the national spatial model across all MESA sites and excluding NY, and boxplot of Ni levels by MESA city. Mean overall Ni

=22.06 ng/m³ (sd 18.40), mean Ni without NY = 14.19ng/m³ (sd 0.65). b) Boxplot of Ni distribution by MESA city. c) Distribution of Chromium across all MESA sites, and boxplot of Cr levels by MESA city. Mean Cr = 19.38 ng/m³ (sd 0.88). d) Boxplot of Cr distribution by MESA city.

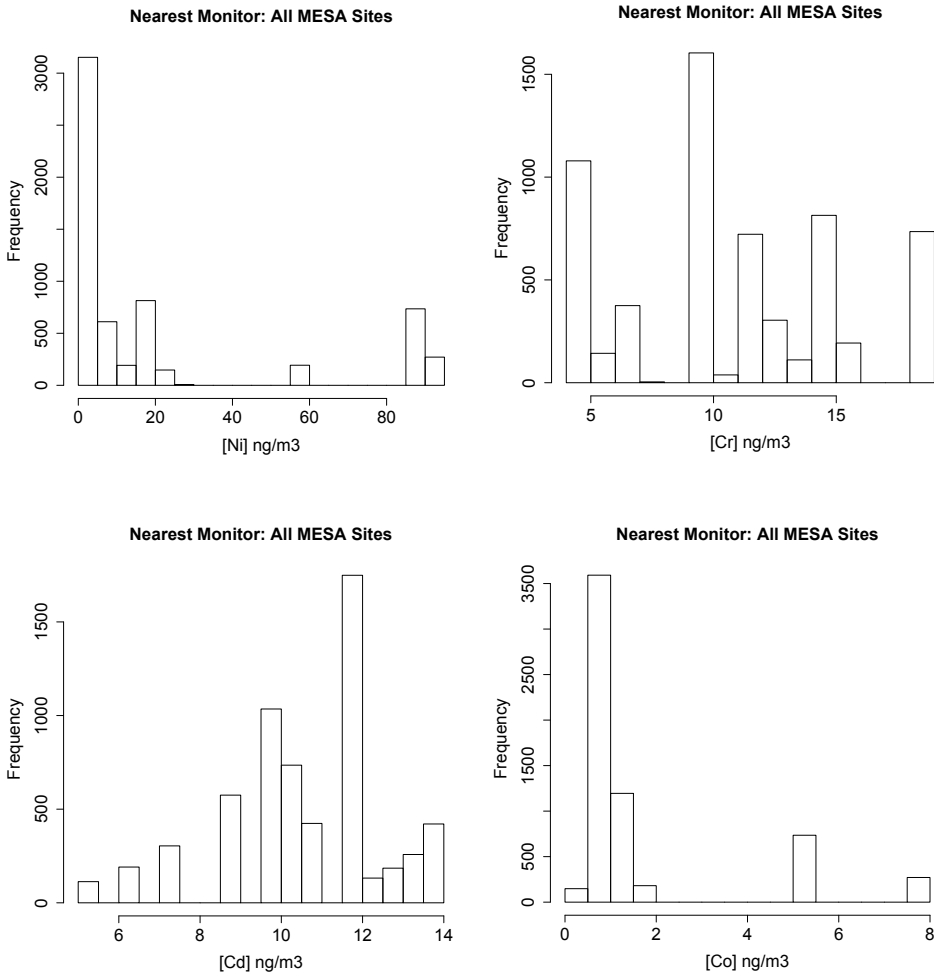


Fig 4. Nearest monitor TM estimates for all MESA sites. Mean Ni = 2.24 ng/m³ (sd 3.16), mean Cr = 1.08ng/m³ (sd 0.43), mean Cd = 1.07 ng/m³ (sd 0.19), mean Co = 0.17ng/m³ (sd 0.19).

Low Attenuation Areas

Low attenuation areas (LAA) ratio were calculated by dividing the number of CT lung tissue voxels with values < -950 HU by the total number of lung voxels. The distribution of this raw LAA ratio was highly right skewed and therefore was log

transformed (logLAA) to approximate a normal distribution. The distribution of logLAA by MESA city is shown in (Fig 5).

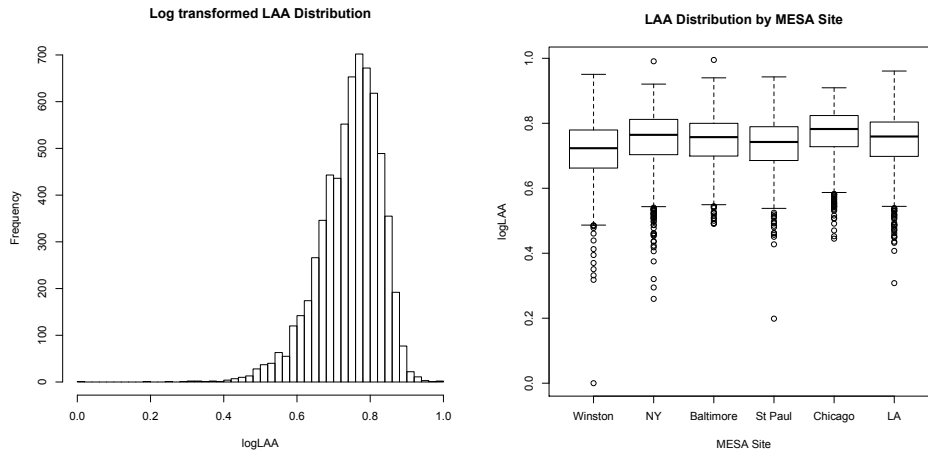


Fig 5. Log transformed distribution of LAA across all sites and by specific MESA city. Mean logLAA 0.744 (sd 0.085)

FEV1 and FEV1/FVC Distribution

Forced Expiratory Volume in 1 second (FEV1) and also the ratio of FEV1 to Forced Expiratory Volume (FEV1/FVC) distributions were examined and found to have a normal distribution and reasonably similar distributions for each MESA city (fig 6). The FEV1 and FEV1/FVC ratio distributions were also compared by gender and race as these are important factors in determining reference ranges for clinical diagnosis (fig 7).

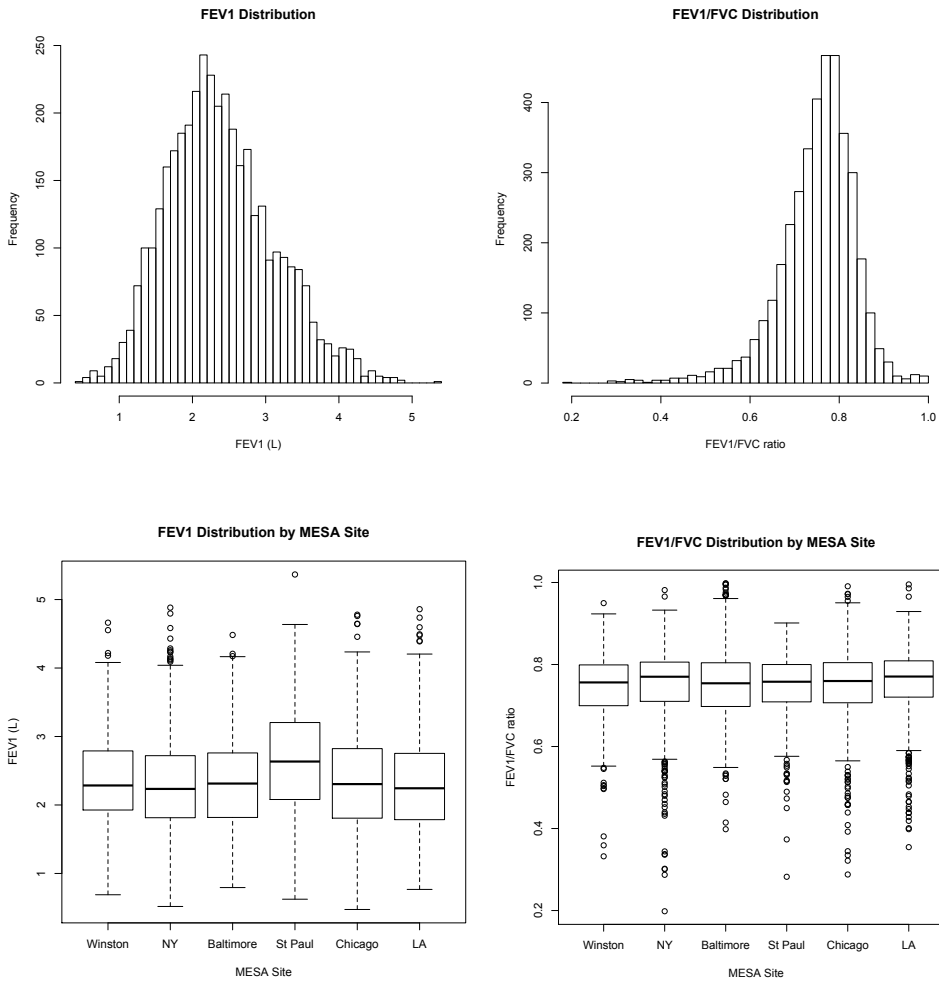
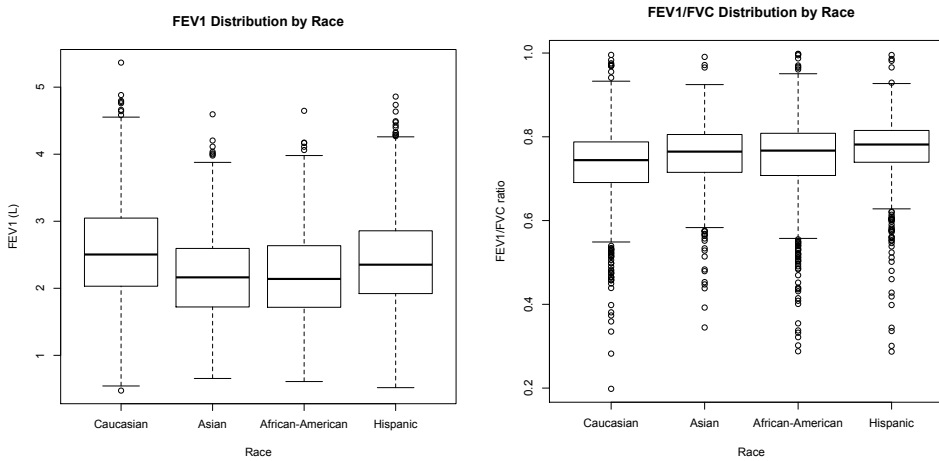


Fig 6. FEV1 and FEV1/FVC distribution across all sites and by specific MESA city. Mean FEV1 = 2.4L (sd 0.73), mean FEV1/FVC ratio = 0.75 (sd 0.086).



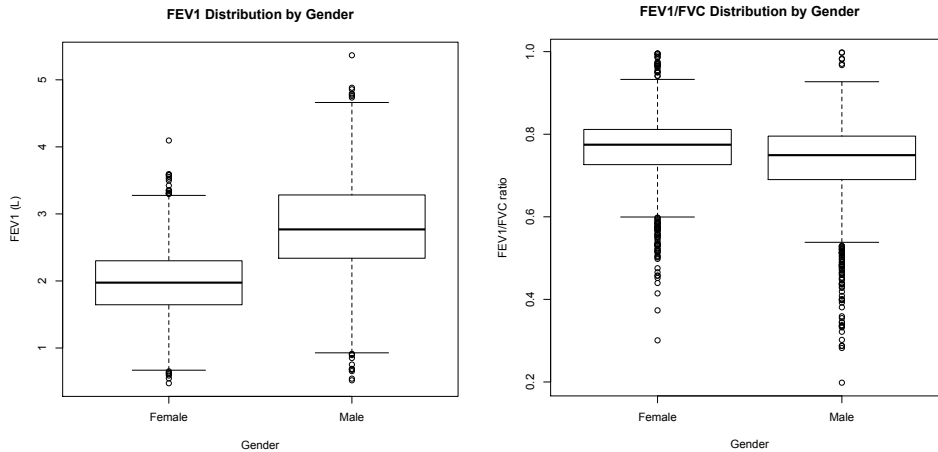


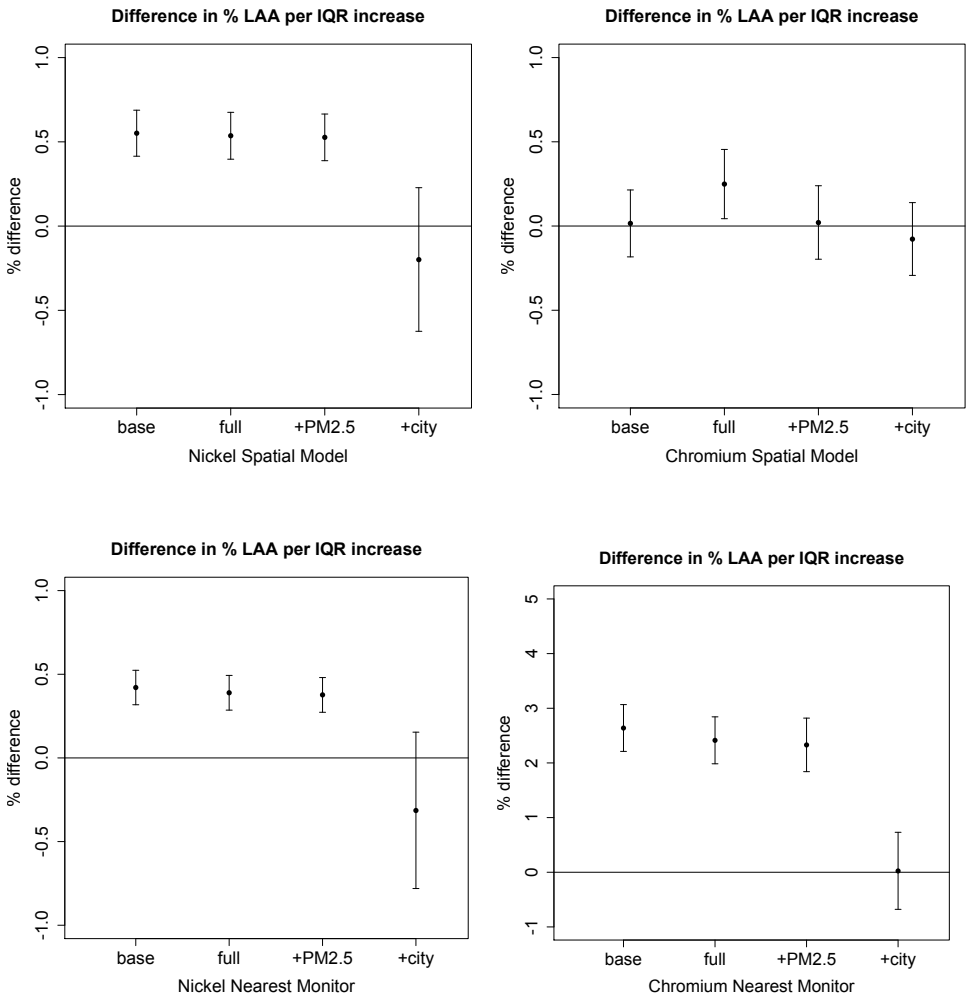
Fig 7. FEV1 and FEV1/FVC stratified by race and gender across all MESA sites.

%LAA Analysis:

Log transformed LAA was regressed on single TM spatial and nearest monitor transition metal estimates for base model (gender, age, height, weight, bmi), full model (base + smoking status, pack years, asthma history, income level, occupation, education) and confounder adjusted models (full model + either PM2.5 or city). Results of these regressions are shown below in effect estimate plots as change in %LAA for an increase in TM IQR.

Spatial Ni model regressions show significance for base, full, and + PM2.5 adjusted models with increase in %LAA for an IQR increase, but not with adjustment by city. By comparison, Cr demonstrated significance in %LAA change per IQR increase only for the full model, but not after PM2.5 adjustment. Nearest monitor regressions for Ni showed similar effect estimates to the spatial model for %LAA difference per IQR increase. The Cr nearest monitor model however was very different from the spatial model as the %LAA increases were significant for each model, and as well larger in effect size. Nearest monitor Cd and Co effects for

all analysis models were also found to have significance though this was lost upon PM2.5 adjustment for Cd. Adjustment for city were non-significant for all spatial and nearest TM models (fig 8). Interestingly TM analysis flipped the effect estimate direction in almost all cases. Spatial Ni estimates were also analyzed for NY estimates, and found to show similar significance for each regression model (full model p-value 3.72e-11, 95%CI 8.19, 15.07). Therefore below we report results only for the full MESA cohort.



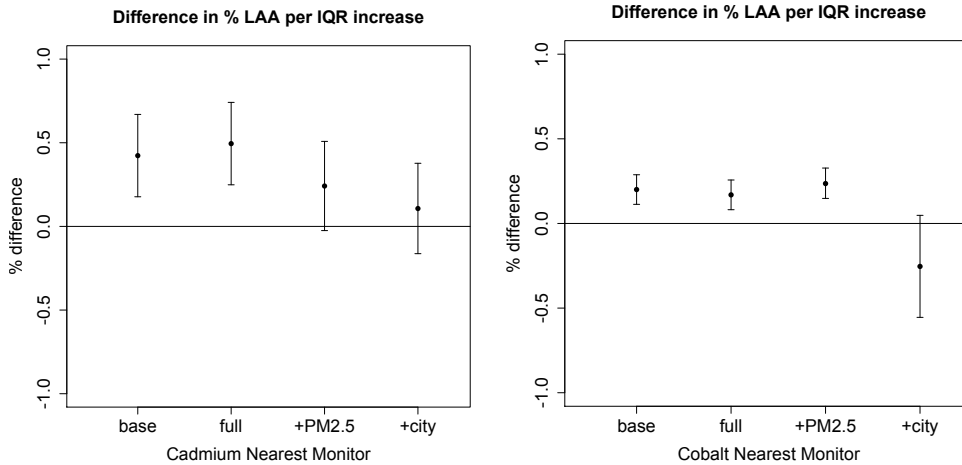


Fig 8. Effect estimate and 95% CI plot for spatial and nearest monitor estimates of Ni, Cr, Cd and Co, showing change in %LAA for a change in IQR comparing models for each TM.

Full models for the spatial and nearest monitor regressions were compared to each other to examine relative effect size for each TM. Side by side comparison shows the similarity for Ni between spatial and nearest monitor estimates, but demonstrate a substantial difference in the Cr effect sizes. The results of Cd and Co nearest monitor estimates are shown for comparison (fig 9).

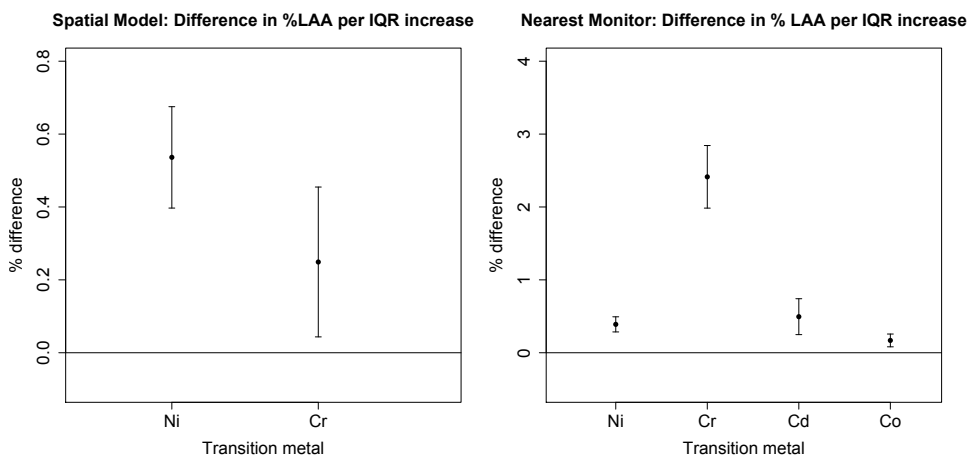


Fig 9. Effect estimate and 95% CI plots show the full model effect of a change in %LAA for an increase in IQR for each TM in the Spatial and Nearest Monitor models.

The full models for the nearest monitor exposures were analyzed using a 2 TM regression approach to assess for confounding by the presence of an additional TM. Comparison of each single TM full model (“unadjusted”) and the 2 TM model (“adjusted”) are shown in fig. 10 below. Findings indicate both Ni and Co effect are lost after Cr adjustment, however Cr and Cd effects do not appear to be significantly influenced by adjustment for a second TM.

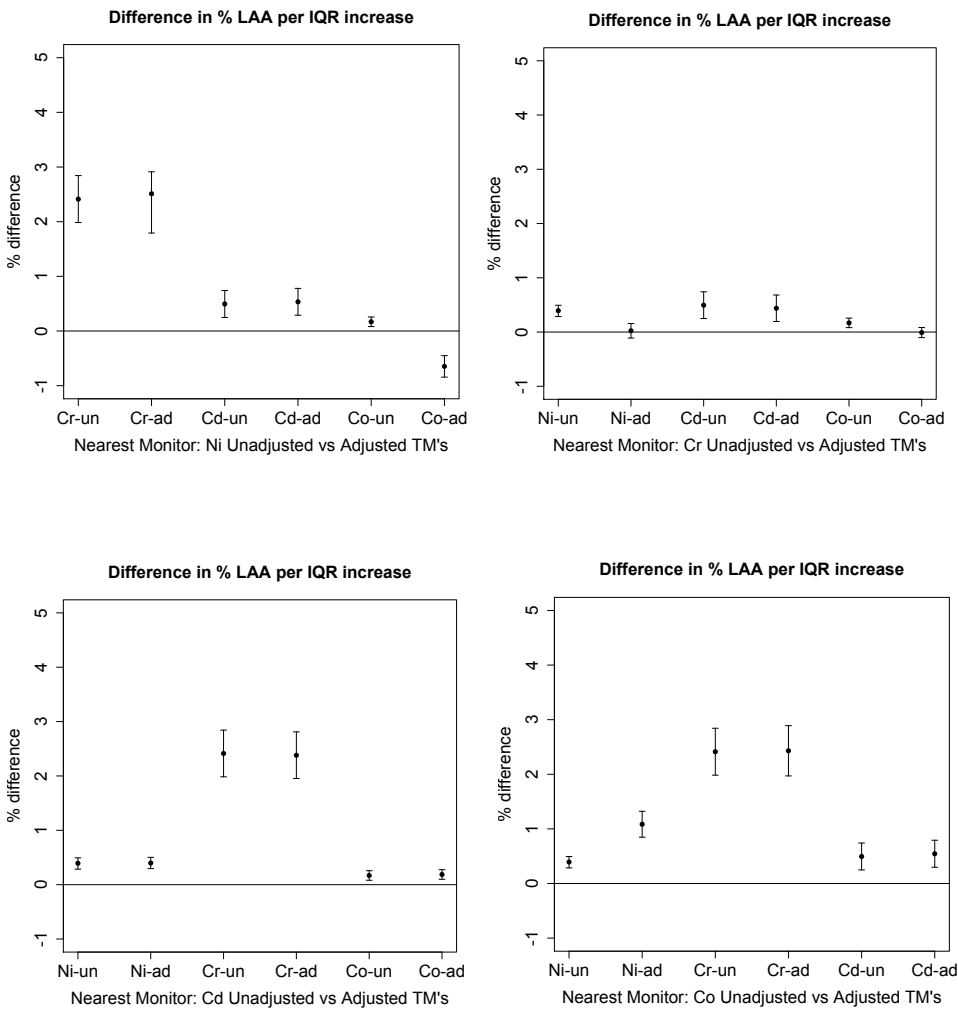


Fig 10. Effect estimate plots for unadjusted full models vs full model + adjusted by a 2nd transition metal, showing the change in %LAA for an increase in IQR for nearest monitor.

FEV1 Analysis:

Analysis for spatial and nearest monitor TM estimates using FEV1 and FEV1/FVC endpoints by base, full, +PM2.5 and + city models were done to investigate coherence with our primary LAA analysis. Below we report the findings only for FEV1 alone as the FEV1/FVC ratio results were similar. For the full models we observed a decrease in %FEV1 volume (L) for each increase IQR in Ni reflecting the findings of the %LAA analysis. This effect was non-significant for Cr in both the spatial and nearest monitor models. Nearest monitor Cd was also non-significant, but was significant for Co full model estimates (fig 11).

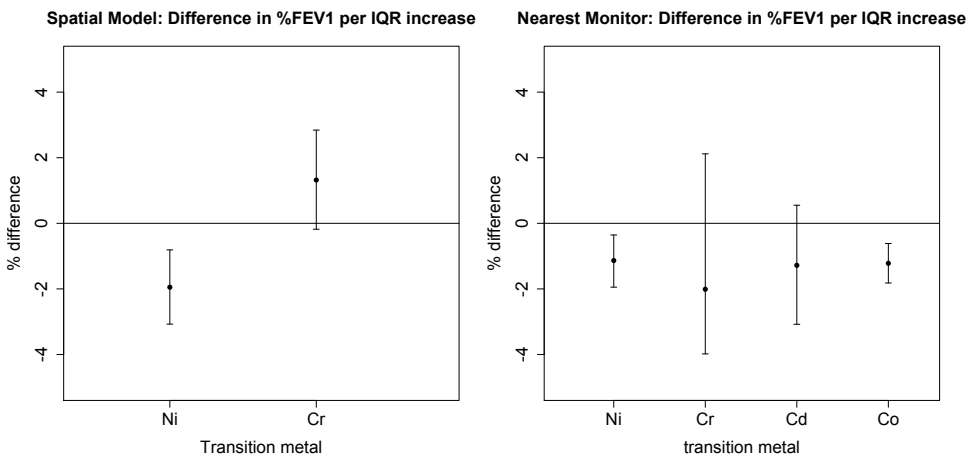
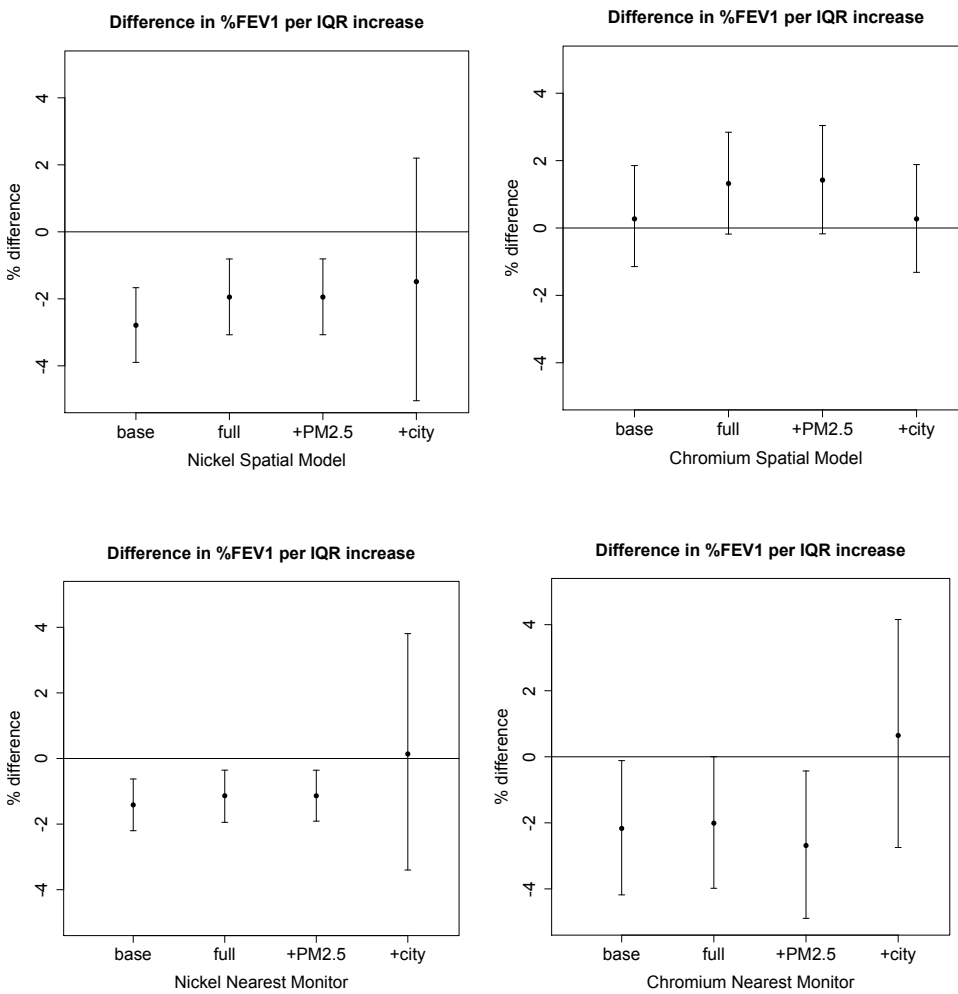


Fig 11. Effect estimate and 95% CI plots show the full model effect of a change in %FEV1 for an increase in IQR for each TM in the Spatial and Nearest Monitor models.

Comparison of spatial and nearest monitor base, full, +PM2.5, and + city models are shown for all TM's. Ni models again demonstrate a decrease in %FEV1 for an IQR increase in similarity to the %LAA analysis. However this was not seen for Cr for the spatial estimates and was marginally significant for nearest monitor full model adjustment. Cd was non-significant for each, and Co showed significant association with decrease in %FEV1 until adjustment for city (fig 12).



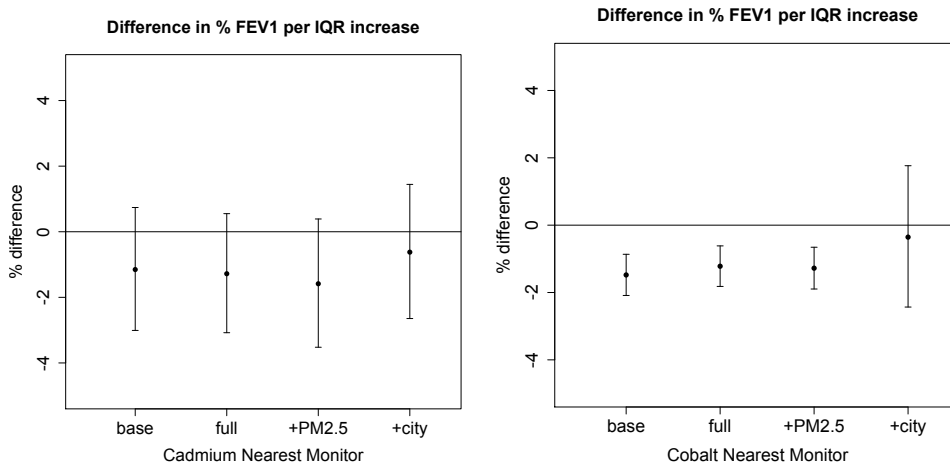


Fig 12. Effect estimate and 95% CI plots for spatial nearest monitor estimates of Ni and Cr, showing change in %LAA for a change in IQR comparing models for each TM.

As with the LAA analysis, full models for the nearest monitor exposures were also analyzed using a 2 TM regression approach to assess for confounding by presence of an additional TM. Comparison of each single TM full model (“unadjusted”) and the 2 TM model (“adjusted”) are shown in fig. 13 below. Findings from this analysis differ from the LAA analysis in that Ni and Co are the only single TM models with associations that remain significant for decrease in %FEV1. Adjustment by Cr slightly lessens the effect of Ni, and the Co effect is relatively unchanged for any 2nd TM adjustment.

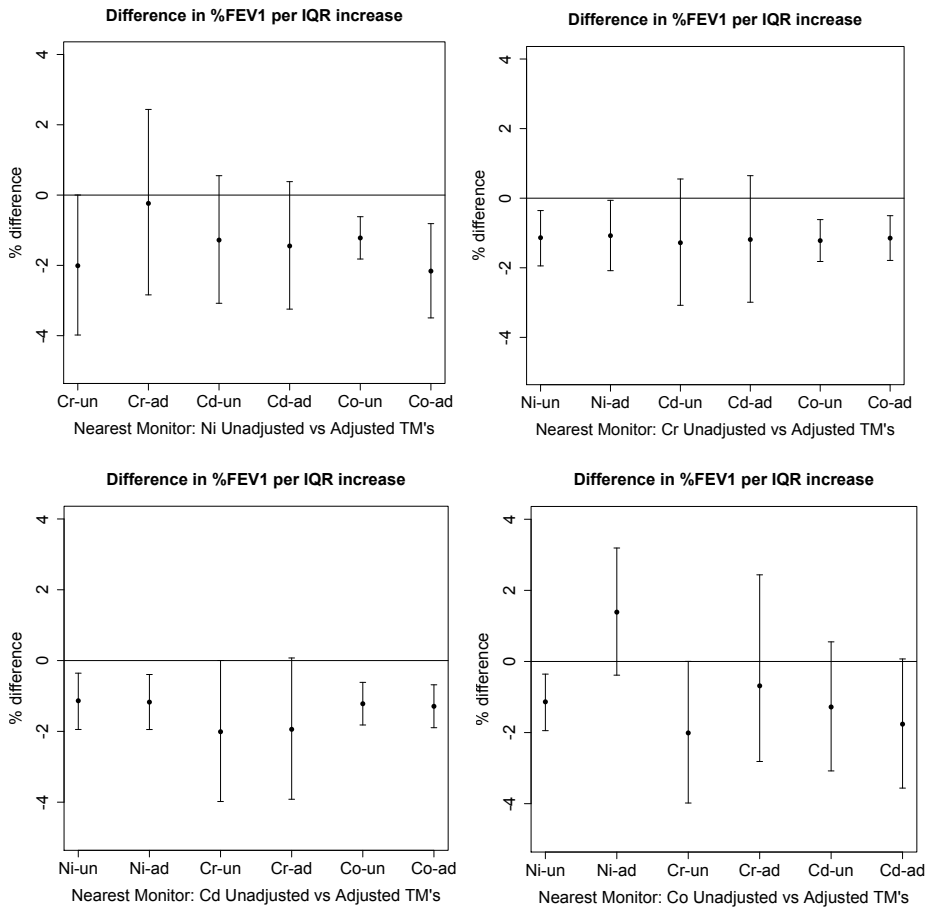


Fig 13- Effect estimate and 95% CI plots for unadjusted full models vs full model + adjusted by a 2nd transition metal, showing the change in %FEV1 for an increase in IQR for nearest monitor.

TM Estimate Correlations:

Overall Ni estimates used for %LAA and %FEV1 analysis show good coherence, however those for Cr analysis do not. This indicates that perhaps the spatial and nearest monitor TM exposure estimates do not correlate well. Spatial vs nearest monitor Ni and Cr estimates were plotted to assess correlation (fig 14). The correlations for Ni were strong ($r = 0.94$), but correlation for Cr was poor ($r = 0.08$).

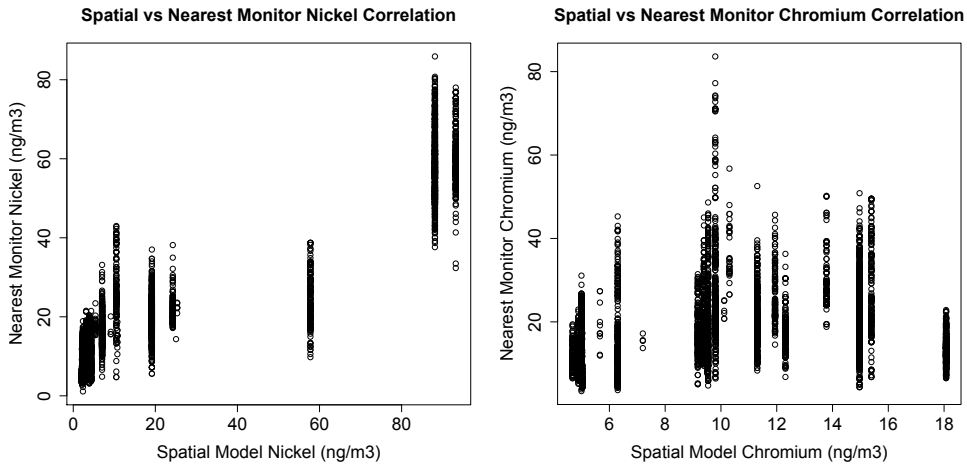
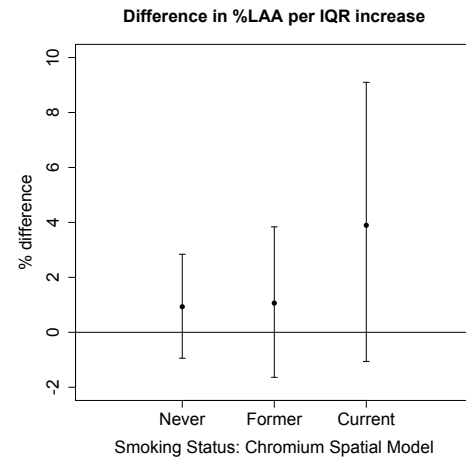
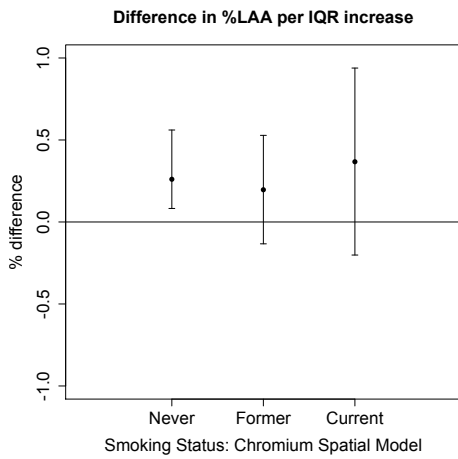
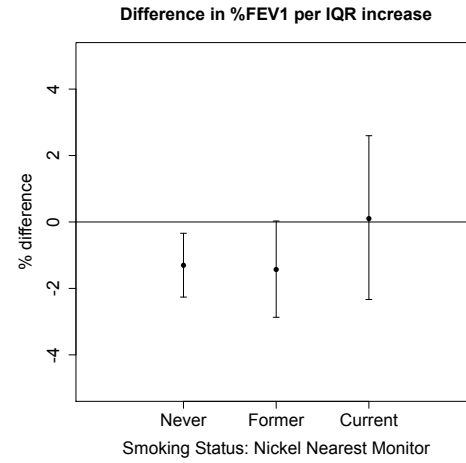
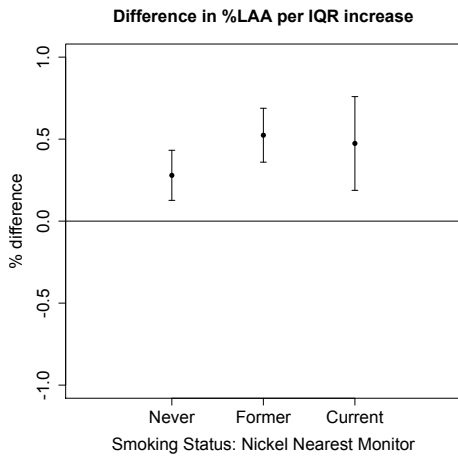
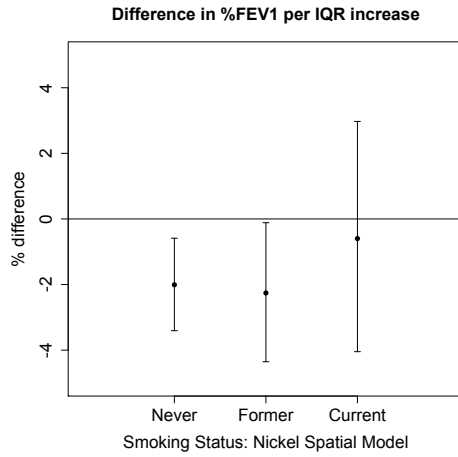
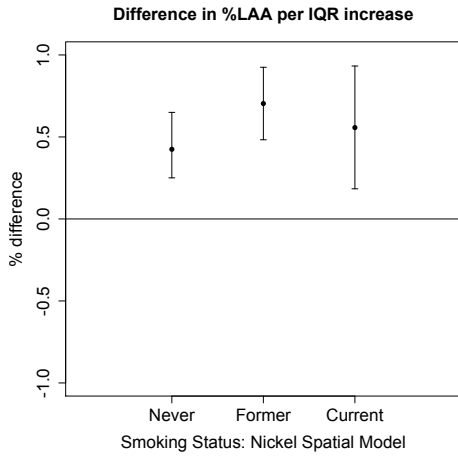


Fig 14. Scatter plots between nearest monitor and spatial TM estimates

Smoking Stratification:

In order to address the known strong effect of smoking on change in %LAA and %FEV1 we stratified the analysis by smoking status category (never, former, and current). Each TM was evaluated by smoking category in both the spatial and nearest monitor estimates and show in fig 15. We observed significant spatial model and nearest monitor full model Ni effect for all smoking status categories in the LAA analysis, but lost effect for current smokers in the %FEV1 analysis. Cr was also significant for effect in each smoking category for only the nearest monitor analysis, but again this effect is lost as well for the %FEV1 endpoint.



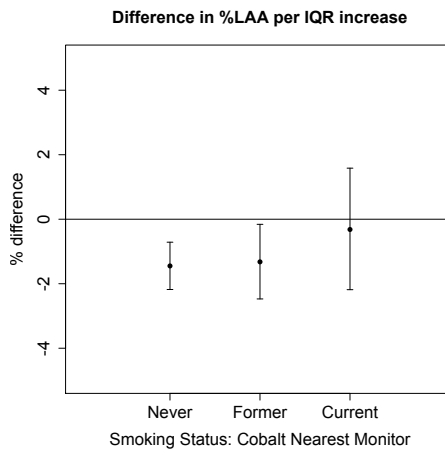
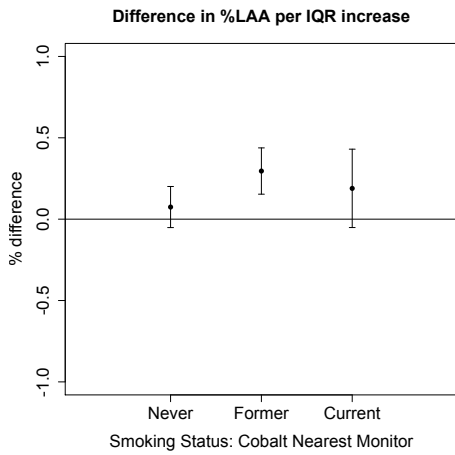
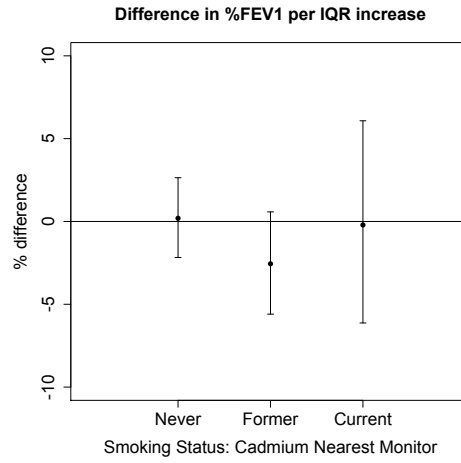
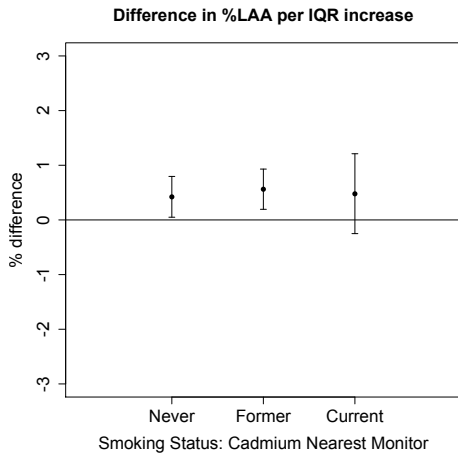
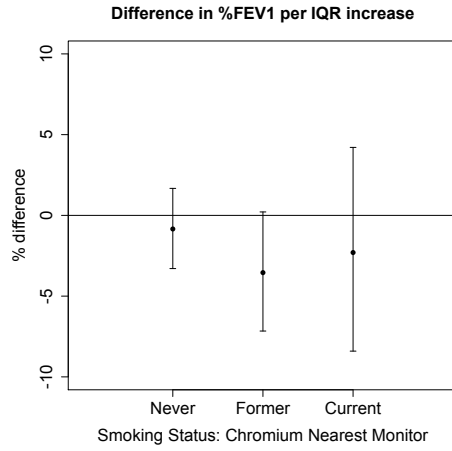
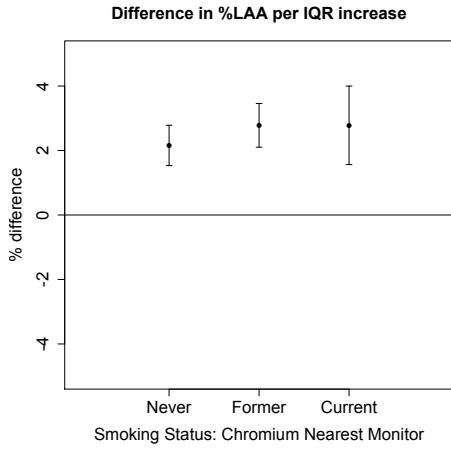


Fig 15. Comparison of effect estimate and 95% CI plots for difference in %LAA and %FEV1 for Ni spatial model and Cr nearest monitor IQR increase stratified by smoking status.

PM2.5 Sensitivity Analysis

LAA and FEV1 endpoints were regressed on fully adjusted models using just PM2.5 estimates in order to determine the effect of this exposure alone. Only a PM2.5 effect on LAA was found to have significance (table 4). Adjustment in this analysis for city showed a non-significant effect of PM.25 (p-value 0.95, 95%CI - 3.50e-05, 1.01e-04).

Models	Estimate	Std. Err	T value	P Value	95% CI	
LAA	2.46e-03	0.38e-03	6.453	1.18e-10	1.71e-03	3.20e-03
FEV1	0.65e-03	2.76e-03	0.236	0.81	-4.77e-03	6.08e-03
FVC	-2.70e-03	3.40e-03	-0.772	0.45	-9.28e-03	4.03e-03
FEV1/FVC	0.78e-03	0.49e-03	1.568	0.12	-0.19e-03	1.74e-03

Table 4. logLAA and Spirometry regression model results for PM2.5 alone.

Discussion

Specific evidence utilizing historical actuary statistics clearly show an increase in mortality secondary to air pollution (AP) and particulate mater (PM) such as from “Fogs of London” dating from the Industrial Revolution in the1700’s, to the infamous “London Fog” of 1952 (32). PM2.5 exposure alone has been demonstrated to have association with decrease in FEV1 in subjects with known chronic pulmonary disease both related to and in the absence of smoking history (33, 34). The association of smoking with increased LAA evident by CT chest

imaging has been investigated in several recent studies (29, 30). To our knowledge, this is the first study investigating the effect of specific PM_{2.5} transition metal components on lung density and function.

The strength of our study design is our access to the large heterogeneous MESA Air cohort, and our use of pre-specified outcomes that correlate well with subclinical and clinical lung disease definitions and diagnostic criteria. Though lung density measurements have not yet been validated as a method for diagnosing and determining severity of obstructive lung disease, quantitative lung CT studies have shown %LAA is strongly correlated with known risk factors such as smoking (22, 25, 29, 30). Our primary hypothesis was to show association between TM exposure estimates and CT lung density as measured by %LAA. This analysis does show significant Ni fully adjusted model association with %LAA increase for both the spatial and nearest monitor estimates, and fully adjusted Cr exposures for the nearest monitor model alone. Cd and Co as well both demonstrate significant association with increase in %LAA for full model adjustment.

Additional strength comes from our secondary hypothesis design using spirometry outcome measures regressed on the same TM exposures in order to show coherence with the primary hypothesis results. This is important as spirometry is the standard clinical method for diagnosis and severity grading of obstructive lung disease based on GOLD criteria (21). Coherence between %LAA and %FEV₁ was well demonstrated with the results of spatial and nearest monitor Ni exposure estimates showing significant and similar effects in all models.

Furthermore, the spatial and nearest monitor Ni exposure estimates correlated well ($r = 0.94$) indicating harmonious analyses.

By comparison we found that %LAA regression on nearest monitor Cr estimates provided stronger significance and larger effects than spatial %LAA regression and for both Cr estimate models for spirometry analysis. Correlation was poor however between the spatial and nearest monitor Cr exposure estimates ($r = 0.084$). We can only surmise that the spatial model using mainly rural based monitors does not accurately reflect the urban Cr distribution and individual exposures within the nearest monitor estimates. Unfortunately Cd and Co estimates were only reliably obtained from the MESA fixed monitors, thus for these metals we were limited to investigating LAA and spirometry associations for the nearest monitor estimates alone. Both Cd and Co were noted to have significant associations for LAA analysis, and only Co showing significance for FEV1 decrease in our spirometry analysis.

Though our primary and secondary hypotheses were designed for coherence, the LAA analysis appears to be more robust than the spirometry analysis. We observed that Ni continued to show significant association between the LAA and FEV1 analyses, however the significant LAA effect of nearest monitor Cr was lost with FEV1 analysis. Furthermore, FEV1 analysis for Ni removing NY subjects also negated significance in the spatial and nearest monitor estimates (data not shown). This may likely reflect decreased power for spirometry analysis as the sample size is much lower ($n=3858$, $n=3056$ without NY subjects) compared to LAA analysis ($n=6545$).

Because PM2.5 is a heterogeneous mixture it was possible that our findings of single TM association with LAA increase and FEV1 decrease may be confounded by the presence of another metal or an exposure outside the scope of this analysis. First we performed an a priori investigation for Ni and Cr full models adjusted by PM2.5 levels and found that this did not meaningfully change the full model results whether these were significant or not. Stratification by smoking status was also done to assess the possible effect of smoking for each TM analysis. We demonstrate that never, former and current smokers all show increase in %LAA per increase in IQR for the nearest monitor Ni and Cr full models. This is less robust for %FEV1 regressed on nearest monitor Ni exposures in never and former smokers, non-significant for current smokers and for all categories for Cr estimates. We did also do post hoc adjustment by adding a second TM to each full model to look for evidence of confounding. Results showed there is likely confounding by presence of a 2nd TM, with only Cr showing robustness to withstand this effect. The full model effect size for %LAA change per nearest monitor Cr IQR increase is noted to be approximately 5x larger than effects for the other metals, and is not changed by adjustment for an additional metal.

Lastly we evaluated whether adjustment for city modified the effects for transition metals on %LAA, Spirometry, and as well for PM2.5 only exposure estimates on these same endpoints. We showed that all effects for both TM and PM2.5 only estimate models were non-significant when adjusting for city. It is not clear that this degree of control is justified. Adjusting for city removes potential confounding by city, but at the price of greatly reducing exposure variability, in

essence turning the analysis into a within-city analysis and ignoring between-city differences in exposure.

This cross-sectional analysis is limited in scope of course as it is only designed to investigate prevalence of subclinical lung disease. Though we do show an association between TM's and prevalent emphysema by CT lung density measurements and spirometry, we are unable to comment on their possible association with incidence and/or progression of lung disease. This is an interesting concept with potential for further analysis using subsequent MESA CT and spirometry values.

Conclusions

We demonstrate clear association of increase in Nickel, Chromium, Cadmium and Cobalt exposure estimates and increase in %LAA by CT lung. This correlation is strongest for both Ni and Cr in the MESA fixed monitor estimates of exposure. This is further supported for Ni exposures in our secondary analysis using spirometry endpoints with demonstrated decrease in %FEV1 for each IQR increase in Ni and Co exposures. This supportive effect was not seen with FEV1 regressed on Cr and Cd, possibly due to lack of sufficient power in the spirometry analysis. PM2.5 adjustment did not demonstrate confounding of TM effect in the spatial and nearest monitor analysis for %LAA analysis. Adjustment by a second TM does demonstrate some confounding effect when comparing our fully adjusted single TM models to those adjusted by a 2nd TM, but Cr alone is robust enough to withstand this effect. Finally, %LAA increase per Ni and Cr IQR increase stratified by smoking status

showed significant association for all categories of smoking, indicating that these TM exposures were independent of this well-known risk factor. We conclude that exposure to Ni, Cr, Cd, and Co components of PM_{2.5} is associated with %LAA increase and suggests independent association with prevalence of obstructive lung disease outside of inheritable, modifiable causes. Further study is needed to assess the association of these and other transition metals with incidence and progression of obstructive lung disease over time.

References:

1. Trends in COPD (Chronic Bronchitis and Emphysema): Morbidity and Mortality. American Lung Association, 2010.
2. Doll R, Hill AB. THE MORTALITY OF DOCTORS IN RELATION TO THEIR SMOKING HABITS - A PRELIMINARY REPORT. *British Medical Journal* 1954;1(4877):1451-5.
3. Doll R, Hill AB. LUNG CANCER AND OTHER CAUSES OF DEATH IN RELATION TO SMOKING - A 2ND REPORT ON THE MORTALITY OF BRITISH DOCTORS. *British Medical Journal* 1956;2(NOV10):1071-81.
4. Hammond EC, Horn D. THE RELATIONSHIP BETWEEN HUMAN SMOKING HABITS AND DEATH RATES - A FOLLOW-UP STUDY OF 187,766 MEN. *Jama-Journal of the American Medical Association* 1954;155(15):1316-28.
5. Moller P, Jacobsen NR, Folkmann JK, et al. Role of oxidative damage in toxicity of particulates. *Free Radical Research* 2010;44(1):1-46.
6. Reff A, Bhave PV, Simon H, et al. Emissions inventory of PM2.5 trace elements across the United States. *Environ Sci Technol* 2009;43(15):5790-6.
7. Barchowsky A, O'Hara KMA. Metal-induced cell signaling and gene activation in lung diseases. *Free Radical Biology and Medicine* 2003;34(9):1130-5.
8. Wallenborn JG, Schladweiler MJ, Richards JH, et al. Differential pulmonary and cardiac effects of pulmonary exposure to a panel of particulate matter-associated metals. *Toxicology and Applied Pharmacology* 2009;241(1):71-80.
9. Valavanidis A, Fiotakis K, Vlachogianni T. Airborne Particulate Matter and Human Health: Toxicological Assessment and Importance of Size and Composition of Particles for Oxidative Damage and Carcinogenic Mechanisms. *Journal of Environmental Science and Health Part C-Environmental Carcinogenesis & Ecotoxicology Reviews* 2008;26(4):339-62.
10. Kawanishi S, Hiraku Y, Murata M, et al. The role of metals in site-specific DNA damage with reference to carcinogenesis. *Free Radical Biology and Medicine* 2002;32(9):822-32.
11. Jomova K, Valko M. Advances in metal-induced oxidative stress and human disease. *Toxicology* 2011;283(2-3):65-87.
12. Niu JJ, Rasmussen PE, Hassan NM, et al. Concentration Distribution and Bioaccessibility of Trace Elements in Nano and Fine Urban Airborne Particulate Matter: Influence of Particle Size. *Water Air and Soil Pollution* 2010;213(1-4):211-25.
13. Stohs SJ, Bagchi D, Bagchi M. Toxicity of trace elements in tobacco smoke. *Inhalation Toxicology* 1997;9(9):867-90.
14. Talhout R, Schulz T, Florek E, et al. Hazardous Compounds in Tobacco Smoke. *International Journal of Environmental Research and Public Health* 2011;8(2):613-28.

15. Kasprzak KS. Oxidative DNA and protein damage in metal-induced toxicity and carcinogenesis. *Free Radical Biology and Medicine* 2002;32(10):958-67.
16. Chen F, Shi XL. Intracellular signal transduction of cells in response to carcinogenic metals. *Critical Reviews in Oncology Hematology* 2002;42(1):105-21.
17. Rennolds J, Butler S, Maloney K, et al. Cadmium Regulates the Expression of the CFTR Chloride Channel in Human Airway Epithelial Cells. *Toxicological Sciences* 2010;116(1):349-58.
18. Denkhaus E, Salnikow K. Nickel essentiality, toxicity, and carcinogenicity. *Critical Reviews in Oncology Hematology* 2002;42(1):35-56.
19. Dick CAJ, Brown DM, Donaldson K, et al. The role of free radicals in the toxic and inflammatory effects of four different ultrafine particle types. *Inhalation Toxicology* 2003;15(1):39-52.
20. Eisner MD, Anthonisen N, Coultas D, et al. An official American Thoracic Society public policy statement: Novel risk factors and the global burden of chronic obstructive pulmonary disease. *Am J Respir Crit Care Med*. United States, 2010:693-718.
21. Gomez FP, Rodriguez-Roisin R. Global initiative for Chronic Obstructive Lung Disease (GOLD) guidelines for chronic obstructive pulmonary disease. *Current Opinion in Pulmonary Medicine* 2002;8(2):81-6.
22. Hoffman EA, Jiang R, Baumhauer H, et al. Reproducibility and Validity of Lung Density Measures from Cardiac CT Scans-The Multi-Ethnic Study of Atherosclerosis (MESA) Lung Study. *Academic Radiology* 2009;16(6):689-99.
23. Carr JJ, Nelson JC, Wong ND, et al. Calcified coronary artery plaque measurement with cardiac CT in population-based studies: Standardized protocol of Multi-Ethnic Study of Atherosclerosis (MESA) and Coronary Artery Risk Development in Young Adults (CARDIA) study. *Radiology* 2005;234(1):35-43.
24. Bild DE, Bluemke DA, Burke GL, et al. Multi-ethnic study of atherosclerosis: objectives and design. *Am J Epidemiol* 2002;156(9):871-81.
25. Lederer DJ, Enright PL, Kawut SM, et al. Cigarette Smoking Is Associated with Subclinical Parenchymal Lung Disease The Multi-Ethnic Study of Atherosclerosis (MESA)-Lung Study. *American Journal of Respiratory and Critical Care Medicine* 2009;180(5):407-14.
26. Mishima M, Hirai T, Itoh H, et al. Complexity of terminal airspace geometry assessed by lung computed tomography in normal subjects and patients with chronic obstructive pulmonary disease. *Proceedings of the National Academy of Sciences of the United States of America* 1999;96(16):8829-34.
27. Mishima M, Itoh H, Sakai H, et al. Optimized scanning conditions of high resolution CT in the follow-up of pulmonary emphysema. *Journal of Computer Assisted Tomography* 1999;23(3):380-4.
28. Gardner RM. STANDARDIZATION OF SPIROMETRY - A SUMMARY OF RECOMMENDATIONS FROM THE AMERICAN THORACIC SOCIETY - THE 1987 UPDATE. *Annals of Internal Medicine* 1988;108(2).

29. Grydeland TB, Dirksen A, Coxson HO, et al. Quantitative computed tomography: emphysema and airway wall thickness by sex, age and smoking. *European Respiratory Journal* 2009;34(4):858-65.
30. Grydeland TB, Dirksen A, Coxson HO, et al. Quantitative Computed Tomography Measures of Emphysema and Airway Wall Thickness Are Related to Respiratory Symptoms. *American Journal of Respiratory and Critical Care Medicine* 2010;181(4):353-9.
31. Peltier RE, Lippmann M. Residual oil combustion: 2. Distributions of airborne nickel and vanadium within New York City. *Journal of Exposure Science and Environmental Epidemiology* 2010;20(4):342-50.
32. Anderson HR. Air pollution and mortality: A history. *Atmospheric Environment* 2009;43(1):142-52.
33. Goss CH, Newsom SA, Schildcrout JS, et al. Effect of ambient air pollution on pulmonary exacerbations and lung function in cystic fibrosis. *American Journal of Respiratory and Critical Care Medicine* 2004;169(7):816-21.
34. Peacock JL, Anderson HR, Bremner SA, et al. Outdoor air pollution and respiratory health in patients with COPD. *Thorax*, 2011.

Appendixes

Appendix A:

Statistical Models:

Base:

1. $\%LAA = B0 + B1(TM) + B2(Race) + B3(Gender) + B4(Age) + B5(Wt) + B6(Ht) + B7(BMI)$
2. $FEV1 = B0 + B1(TM) + B2(Race) + B3(Gender) + B4(Age) + B5(Wt) + B6(Ht) + B7(BMI)$
3. $FEV1/FVC = B0 + B1(TM) + B2(Race) + B3(Gender) + B4(Age) + B5(Wt) + B6(Ht) + B7(BMI)$

Full:

4. $\%LAA = \text{Base Model} + B8(Pkyrs) + B9(Smkst) + B10(asth) + B11(occupation) + B12(income) + B13(education)$
5. $FEV1 = \text{Base Model} + B8(Pkyrs) + B9(Smkst) + B10(asth) + B11(occupation) + B12(income) + B13(education)$
6. $FEV1/FVC = \text{Base Model} + B8(Pkyrs) + B9(Smkst) + B10(asth) + B11(occupation) + B12(income) + B13(education)$

Confounder Adjusted:

7. $\%LAA = \text{Full Model} + B14(PM2.5 \text{ or City})$

8. FEV1 = Full Model + B14(PM2.5 or City)

9. FEV1/FVC = Full Model + B14(PM2.5 or City)

Appendix B:

Power Calculation and Formulae

$\text{Pwr.f2.test}(u = \# \text{predictors} - 1, v = \text{sample size} - \# \text{predictors}, f2 = \text{effect size}, \text{sig.level} = 0.05, \text{power} = 0.5, 0.8, 0.9)$

$$F2 = R^2_{\text{total}} - R^2_{\text{model}} / 1 - R^2_{\text{total}}$$

Rearranged to solve for R^2_{total} :

$$R^2_{\text{total}} = (R^2_{\text{model}} + F2) / (1 + F2)$$

R^2_{total} = Value obtained in full model analysis

$R^2_{\text{model}} = 0.2159$ from Grydeland et al (30)

Detectable % difference is $X = R^2_{\text{total}} - R^2_{\text{model}} \times 100$.